

Continuum generation by dark solitons

C. Milián^{1,2}, D.V. Skryabin^{1,*}, A. Ferrando³

¹*Centre for Photonics and Photonic Materials, Department of Physics, University of Bath,
Bath BA2 7AY, UK*

²*Instituto ITACA, Universidad Politécnica de Valencia, Camino de Vera S/N, 46022
Valencia, Spain*

³*Departamento de Óptica, Interdisciplinary Modeling Group InterTech, Universidad de
Valencia, Dr. Moliner 50, 46100 Burjassot, Valencia, Spain*

**Corresponding author: d.v.skryabin@bath.ac.uk*

We demonstrate that the dark soliton trains in optical fibers with a zero of the group velocity dispersion can generate broad spectral distribution (continuum) associated with the resonant dispersive radiation emitted by solitons. This radiation is either enhanced or suppressed by the Raman scattering depending on the sign of the third order dispersion. © 2018 Optical Society of America

OCIS codes: 000.0000, 999.9999.

One of many fundamental and practical outcomes of research into supercontinuum generation in optical fibers [1, 2] has been a change of emphasis in studies of temporal solitons. If in the pre-supercontinuum era fiber solitons were mostly perceived as information carriers [3], now days they are widely recognized and researched as facilitators and mediators of efficient frequency conversion in infrared and visible parts of spectrum [1, 2].

Trains of bright solitons naturally emerge in fibers from an intense pump pulse and their role in supercontinuum generation and frequency conversion has been extensively explored [1, 2]. In particular, it has been demonstrated that the interplay of the Raman scattering and third order dispersion (TOD) can lead to the exponential amplification of the resonant (Cherenkov) radiation emitted by a soliton [4]. This happens if the central soliton frequency is shifted by the Raman effect towards a zero of the group velocity dispersion (GVD), which is possible if TOD is negative [4]. Amplification of the resonant radiation has been used to create coherent infrared fiber based sources [5–7]. While, the widest octave broad supercontinua extended from $\sim 400\text{nm}$ to $\sim 2\mu\text{m}$ have been most commonly observed across the zero GVD point with positive TOD [8]. Generation of these spectra is fueled by the cascaded scattering of the short wavelength radiation on and its trapping by the Raman solitons [2, 9, 10].

Theory of the radiation emission by bright solitons has been developed well before the recent wave of supercontinuum research [1, 11]. However, importance of the Raman effect in the soliton-radiation interaction has been revealed and explained only recently [4, 9]. Similarly, it is known that *dark solitons* also emit radiation when perturbed by TOD [12, 13], but the interplay of this process with the Raman scattering has not been studied so far and is the subject of this Letter. Trains of dark solitons can be created with the established methods [14, 15] and, as we will demonstrate below, can generate continuum of dispersive radiation. Continuum generation by dark solitons can be important not only from a fundamental point of view, but also practically relevant if the pump frequency is in the normal GVD range of a fiber and generation of a broadband signal across the zero GVD wavelength is sought.

A model we use is the dimensionless NLS equation with the TOD and Raman terms

$$i\partial_z A = \frac{1}{2}\partial_t^2 A + i\epsilon\partial_t^3 A - (1 - \theta)|A|^2 A - \theta A \int R(t')|A(t - t')|^2 dt'. \quad (1)$$

Here R is the Raman response function of silica and $\theta = 0.18$ [1]. t is the delayed time measured in the units of $T = 100\text{fs}$. $\epsilon = \beta_3/[6T\beta_2]$ is a small parameter characterizing the ratio between TOD (β_3) and normal GVD ($\beta_2 > 0$). A is the amplitude of the electric field scaled to \sqrt{P} , where $P = 1/[\gamma L_D]$. $L_D = T^2/\beta_2$ is the dispersion length and γ is the nonlinear fiber parameter. Assuming $A \sim e^{-i\delta t}$, the zero GVD frequency is $\delta_0 = -1/[6\epsilon]$. For positive (or negative) TOD the anomalous GVD range hostile to the existence of dark solitons is located for $\delta < \delta_0$ (or $\delta > \delta_0$). A unit of δ corresponds to 10THz.

We are interested in A consisting of the dark soliton F plus small radiation g : $A(z, t) = (F(\tau, z) + g(\tau, z))e^{i\kappa^2 z}$, where $\tau = t - z\kappa \sin \phi$. The soliton solution is [16]

$$F = \kappa \tanh[\tau\kappa \cos \phi] \cos \phi - i\kappa \sin \phi. \quad (2)$$

$\kappa > 0$ is the amplitude of the soliton background. ϕ is the darkness parameter, with the condition $\cos \phi \geq 0$ implying $\phi \in [-\pi/2, \pi/2]$. $\phi = 0$ corresponds to the black soliton having zero amplitude in the middle and propagating with the group velocity matching the background velocity [16]. $\phi \in (0, \pi/2)$ and $\phi \in (-\pi/2, 0)$ correspond to the dark solitons propagating, respectively, slower and faster than the background wave.

Solutions of a linearized equation for g are sought in the form

$$g = G_1 e^{i\delta_r \tau - i\lambda z - i\phi} + G_2^* e^{-i\delta_r \tau + i\lambda z + i\phi}. \quad (3)$$

Note, that for $A \sim e^{-i\delta t}$, the exponent $e^{i\delta_r \tau}$ with $\delta_r > 0$ corresponds to the overall negative frequency shift. Condition $\lambda = 0$ leads to the resonant frequency [12, 13]

$$\delta_r^2 = \frac{1}{2\epsilon^2} [\alpha + \sqrt{\alpha^2 + 4\kappa^2 \epsilon^2 \cos^2 \phi}], \quad \alpha \equiv 2\epsilon\kappa \sin \phi + \frac{1}{4}. \quad (4)$$

Expanding in ϵ we find $\delta_r = 1/(2\epsilon)(1 + 4\kappa\epsilon \sin \phi + 2\kappa^2\epsilon^2 \cos^2 \phi + O(\epsilon^3))$, so that $|\delta_r| > |\delta_0|$, i.e. the resonant frequency is detuned further away from the soliton, than the zero GVD frequency. An important difference with bright solitons is that the amplitudes G_1 and G_2 are not independent here, but are coupled by nonlinear interaction mediated by the finite amplitude soliton background. The ratio of these amplitudes works out as

$$\frac{G_1}{G_2} = -\frac{1}{\epsilon^2\kappa^2} \left[\frac{1 + 4\kappa\epsilon \sin \phi + O(\epsilon^2)}{1 + 7 \sin^2 \phi} \right]. \quad (5)$$

Eq. (3) implies that the radiation spectrum is expected to peak on both sides from the soliton spectral center at $\delta = 0$. Since $|\delta_r| > |\delta_0|$, one of the radiation peaks belongs to the normal GVD range and the other one to the anomalous GVD. From Eq. (5) it follows that the amplitude of the radiation belonging to the anomalous GVD range is much larger. The above holds for both signs of TOD, i.e. ϵ . Thus the radiation is primarily emitted into a spectral range where the balance of GVD and nonlinearity is not able to support dark solitons. Figs. 1(a,b) show solitons and their radiation using XFROG spectrograms [1] calculated with the Raman effect disregarded ($\theta = 0$). For $\epsilon > 0$ (Fig. 1(a)) and $\epsilon < 0$ (Fig. 1(b)) the strong and weak radiation peaks are swapped, so that the strong one always belongs to the anomalous GVD range. Spectrograms used here are computed as $S(\delta, t) = |\int A(t') \text{sech}(t' - t) \exp[-i\delta t'] dt'|^2$. For $\kappa \cos \phi = 1$ and $t = 0$ the dark soliton spectrogram, $A = F$, can be calculated explicitly

$$S \propto (\delta^2 \cos^2 \phi + 2\delta \sin \phi \cos \phi + \sin^2 \phi) \text{sech}^2[\pi\delta/2]. \quad (6)$$

Taking account of the Raman scattering significantly changes the radiation pattern, cf. Fig. 1 and Fig. 2. The Raman effect enhances both radiation peaks for positive TOD and suppresses them for negative TOD. Physics behind this observation is as follows. Spectrogram $S(\delta, 0)$ of the ideal black, $\phi = 0$, soliton consists of the two symmetric in δ peaks (not clearly seen in Fig. 1, but obvious from Eq. (6)). It means that the resonant radiation in the anomalous GVD range is excited by the black soliton with equal efficiency for either positive or negative TOD. The Raman scattering however transfers more energy into the lower frequency ($\delta < 0$) side of the soliton spectrum. It makes more of the soliton energy to flow into the anomalous GVD range, providing TOD is positive. For negative TOD, however, the effective spectral center of mass of the soliton is shifted by the Raman effect further into the normal GVD range, where little disturbs the balance of normal GVD and nonlinearity. Naturally, this depletes the energy transfer into radiation. Asymmetry of the dark soliton spectra induced by the Raman effect assumed in the above discussion can be readily verified numerically and was experimentally measured 20 years ago [17].

The soliton spectral asymmetry induced by the Raman scattering can be mimicked by taking the fast dark solitons ($\phi < 0$), see Eq. (6). Equally it is true to say, that the Raman

scattering accelerates dark solitons by inducing the adiabatic drift of ϕ in the direction of $-\pi/2$. Thus by taking initially a faster (slower) soliton in a positive (negative) TOD fiber one shifts more of the soliton energy to the anomalous GVD range, thereby boosting energy transfer into dispersive radiation. This point is further discussed and illustrated below.

A train of dark solitons is an obvious candidate for generation of multiple radiation peaks forming a continuous spectrum. One of the straightforward ways to generate these trains is through the dispersion induced interference of two suitably delayed short pulses [14, 15]. Each interference dip has its own carrier frequency associated with the chirp developing across the whole interference pattern. The characteristic GVD and nonlinear lengths can be made approximately equal and are typically shorter than the TOD length. Thus one can arrange initial conditions so that the solitons are formed first and then the TOD induced radiation starts to develop.

Fig. 3 shows time domain evolution of the soliton train for $\epsilon > 0$ (a) and for $\epsilon < 0$ (b). Both are with the Raman effect included. The solitons are separated into two groups. The ones found for $t < 0$ and $t > 0$ are the fast ($\phi < 0$) and slow ($\phi > 0$) solitons, respectively. For $\epsilon > 0$ the spectra of the fast solitons are shifted towards the range of anomalous GVD. Therefore these solitons are more keen to emit radiation, than the slow solitons (see pronounced oscillations developing for $t < 0$ in Fig. 3(a)). The Raman effect enhances the soliton spectral asymmetry further and boosts the radiation emission by the fast solitons, see Fig. 3(b). For $\epsilon < 0$ spectra of the slow solitons have greater overlap with the anomalous GVD range. However, the Raman effects tends to compensate for this. Thus the net effect is the radiation depletion, cf. Fig. 3(a) and (b).

Spectral evolution along the fiber length for the cases of positive and negative TOD corresponding to the time plots in Fig. 3 are shown in Fig. 4. Far stronger energy transfer from the normal to the anomalous GVD range is obvious in the positive TOD case. Quantitative characterization of this effect is facilitated by Fig. 5, where the full lines show the spectral distributions (plotted using the log-scale) corresponding to the final time domain signals in Fig. 3. The spectrum generated in the anomalous GVD range is few orders of magnitude stronger, than the one in the negative TOD case. Contrary, if the Raman effect is switched off, then $\epsilon > 0$ case is a mirror image of the $\epsilon < 0$ case, cf. the dashed lines in Fig. 5(a) and (b).

In summary, we have demonstrated that the Raman scattering significantly amplifies resonant dispersive radiation emitted by a train of dark solitons in fibers with the positive third order dispersion. This leads to generation of a broad band continuum in the anomalous GVD range, when a pair of pump pulses is applied in the normal GVD. Practical realizations of this effect and its applications for frequency conversion should be investigated further.

CM gratefully thanks the Formacin de Profesorado Universitario predoctoral grant. DVS

is grateful to A. Yulin and J. Dudley for early inputs.

References

1. J. M. Dudley, G. Genty, and S. Coen, *Rev. Mod. Phys.* **78**, 1135 (2006).
2. J. C. Knight and D. V. Skryabin, *Opt. Express* **15**, 15365 (2007).
3. L. Mollenauer and J. Gordon, *Solitons in Optical Fibers: Fundamentals and Applications* (Academic Press, 2006).
4. D. V. Skryabin, F. Luan, J. C. Knight, and P. S. Russell, *Science* **301**, 1705 (2003).
5. P. Falk, M. H. Frosz, O. Bang, L. Thrane, P. E. Andersen, A. O. Bjarklev, K. P. Hansen, and J. Broeng, *Opt. Lett.* **33**, 621 (2008).
6. B. W. Liu, M. L. Hu, X. H. Fang, Y. F. Li, L. Chai, C. Y. Wang, W. J. Tong, J. Luo, A. A. Voronin, and A. M. Zheltikov, *Opt. Express* **16**, 14987 (2008).
7. C. Zhigang, A. Efimov, and A. J. Taylor, *Opt. Express* **17**, 5852 (2009).
8. J. K. Ranka, R. S. Windeler, and A. J. Stentz, *Opt. Lett.* **25**, 25 (2000).
9. A. V. Gorbach and D. V. Skryabin, *Nature Photonics* **1**, 653 (2007).
10. B. A. Cumberland, J. C. Travers, S. V. Popov, and J. R. Taylor, *Opt. Lett.* **33**, 2122 (2008).
11. P. K. A. Wai, H. H. Chen, and Y. C. Lee, *Phys. Rev. A* **41**, 426 (1990).
12. V. I. Karpman, *Phys. Lett. A* **181**, 211 (1993).
13. V. V. Afanasjev, Y. S. Kivshar, and C. R. Menyuk, *Opt. Lett.* **21**, 1975 (1996).
14. J. E. Rothenberg, *Opt. Commun.* **82**, 107 (1991).
15. J. E. Rothenberg and H. K. Heinrich, *Opt. Lett.* **17**, 261 (1992).
16. Y. S. Kivshar and B. Luther-Davies, *Phys. Rep.* **298**, 81 (1998).
17. A. M. Weiner, R. N. Thurston, W. J. Tomlinson, J. P. Heritage, D. E. Leaird, E. M. Kirschner, and R. J. Hawkins, *Opt. Lett.* **14**, 868 (1989).

References

1. J. M. Dudley, G. Genty, and S. Coen, 'Supercontinuum generation in photonic crystal fiber', *Rev. Mod. Phys.* **78**, 1135 (2006).
2. J. C. Knight and D. V. Skryabin, 'Nonlinear waveguide optics and photonic crystal fibers', *Opt. Express* **15**, 15365 (2007).
3. L. Mollenauer and J. Gordon, *Solitons in Optical Fibers: Fundamentals and Applications* (Academic Press, 2006).
4. D. V. Skryabin, F. Luan, J. C. Knight, and P. S. Russell, 'Soliton self-frequency shift cancellation in photonic crystal fibers', *Science* **301**, 1705 (2003).
5. P. Falk, M. H. Frosz, O. Bang, L. Thrane, P. E. Andersen, A. O. Bjarklev, K. P. Hansen, and J. Broeng, 'Broadband light generation at similar to 1300 nm through spectrally recoiled solitons and dispersive waves', *Opt. Lett.* **33**, 621 (2008).
6. B. W. Liu, M. L. Hu, X. H. Fang, Y. F. Li, L. Chai, C. Y. Wang, W. J. Tong, J. Luo, A. A. Voronin, and A. M. Zheltikov, 'Stabilized soliton self-frequency shift and 0.1-PHz sideband generation in a photonic-crystal fiber with an air-hole-modified core', *Opt. Express* **16**, 14987 (2008).
7. C. Zhigang, A. Efimov, and A. J. Taylor, 'Coherent mid-infrared broadband continuum generation in non-uniform ZBLAN fiber taper', *Opt. Express* **17**, 5852 (2009).
8. J. K. Ranka, R. S. Windeler, and A. J. Stentz, 'Visible continuum generation in air-silica microstructure optical fibers with anomalous dispersion at 800 nm', *Opt. Lett.* **25**, 25 (2000).
9. A. V. Gorbach and D. V. Skryabin, 'Light trapping in gravity-like potentials and expansion of supercontinuum spectra in photonic-crystal fibres', *Nature Photonics* **1**, 653 (2007).
10. B. A. Cumberland, J. C. Travers, S. V. Popov, and J. R. Taylor, 'Toward visible cw-pumped supercontinua', *Opt. Lett.* **33**, 2122 (2008).
11. P. K. A. Wai, H. H. Chen, and Y. C. Lee, 'Radiations by solitons at the zero group-dispersion wavelength of single-mode optical fibers', *Phys. Rev. A* **41**, 426 (1990).
12. V. I. Karpman, 'Stationary and radiating dark solitons of the 3rd-order nonlinear Schrodinger-equation', *Phys. Lett. A* **181**, 211 (1993).
13. V. V. Afanasjev, Y. S. Kivshar, and C. R. Menyuk, 'Effect of third-order dispersion on dark solitons', *Opt. Lett.* **21**, 1975 (1996).
14. J. E. Rothenberg, 'Dark soliton trains formed by visible pulse collisions in optical fibers', *Opt. Commun.* **82**, 107 (1991).
15. J. E. Rothenberg and H. K. Heinrich, 'Observation of the formation of dark-soliton trains in optical fibers', *Opt. Lett.* **17**, 261 (1992).

16. Y. S. Kivshar and B. Luther-Davies, 'Dark optical solitons: physics and applications', *Phys. Rep.* **298**, 81 (1998).
17. A. M. Weiner, R. N. Thurston, W. J. Tomlinson, J. P. Heritage, D. E. Leaird, E. M. Kirschner, and R. J. Hawkins, 'Temporal and spectral self-shifts of dark optical solitons', *Opt. Lett.* **14**, 868 (1989).

Figure captions

Fig. 1. (Color online) XFROG spectrograms showing resonant radiation by a dark soliton without the Raman effect ($\theta = 0$). Dashed vertical lines indicate $\pm\delta_r$ predicted by Eq. (4). Full vertical lines indicate the zero GVD frequency δ_0 . (a) $\epsilon = 0.0833$ and (b) $\epsilon = -0.0833$. Other parameters are $\kappa = 1$, $\phi = 0$, $z = 30$.

Fig. 2. (Color online) The same as Fig. 1, but with the Raman effect ($\theta = 0.18$). Strong emission of radiation by the black soliton, see (a), is accompanied by creation of a shallow dark soliton with ϕ close $-\pi/2$ (marked with an arrow).

Fig. 3. (a) Time domain evolution of the dark soliton train in a fiber with positive TOD: $\epsilon = 0.0217$, $\theta = 0.18$. Initial condition is $A = \sqrt{10}[\text{sech}(t - 3) + \text{sech}(t + 3)]$. (b) is the same as (a), but for negative TOD: $\epsilon = -0.0217$.

Fig. 4. (Color Online) Spectral development of continuum generation by a train of dark solitons corresponding to the time domain evolution in Fig. 3, but for larger z . Full vertical lines indicate the zero GVD frequency.

Fig. 5. Full lines in (a) and (b) show spectra corresponding to the $z = 10$ time domain signals in Fig. 3. Dashed lines show the corresponding spectra computed without the Raman effect ($\theta = 0$).

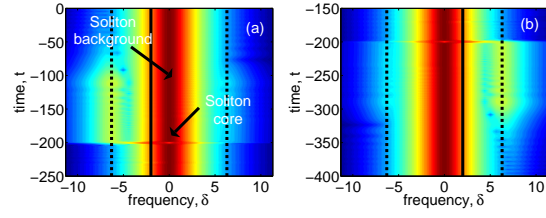


Fig. 1.

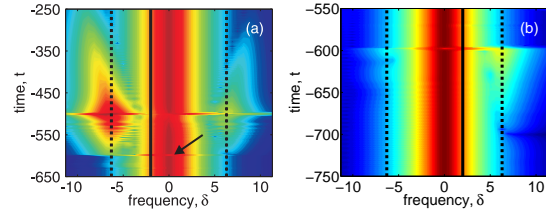


Fig. 2.

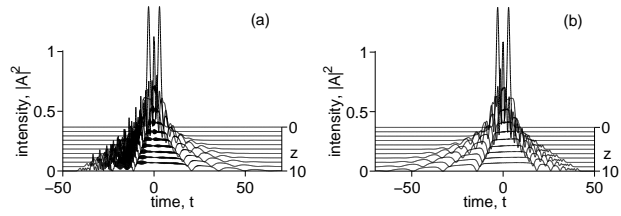


Fig. 3.

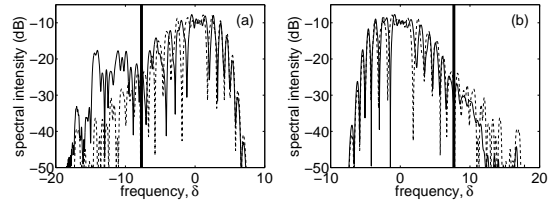


Fig. 4.

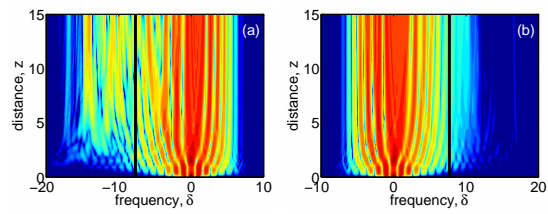


Fig. 5.